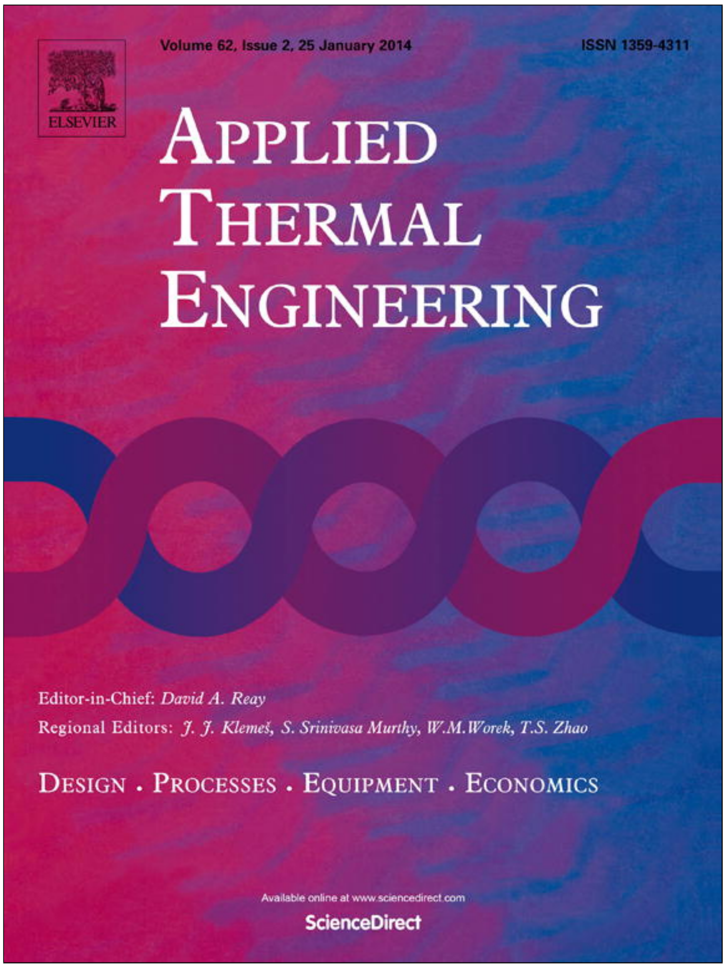
Volume 62, Issue 2, 25 January 2014
ISSN 1359-4311
ELSEVIER
APPLIED
THERMAL
ENGINEERING
Editor-in-Chief: David A. Reay
Regional Editors: J. J. Klemeš, S. Srinivasa Murthy, W.M.Worek, T.S. Zhao
DESIGN . PROCESSES . EQUIPMENT . ECONOMICS
Available online at www.sciencedirect.com
ScienceDirect

Applied Thermal Engineering 62 (2014) 545–552

Contents lists available at ScienceDirect

Applied Thermal Engineering

journal homepage: www.elsevier.com/locate/apthermeng

A fast and simple numerical model for a deeply buried underground tunnel in heating and cooling applications

Xichen Liu [a,b], Yimin Xiao [a,*], Kiao Inthavong [b], Jiyuan Tu [b]

[a] College of Urban Construction and Environmental Engineering, Chongqing University, No. 83, North Street, Shapingba District, Chongqing 400045, China
[b] School of Aerospace, Mechanical and Manufacturing Engineering, RMIT University, PO Box 71, Bundoora, VIC 3083, Australia

HIGHLIGHTS

- A high efficient numerical model for underground tunnel ventilation is proposed.
- The model describe the heat transfer and taking into account condensation.
- A set of discrete numerical equations and its solution method is proposed.
- The model greatly simplified computational difficulty and reduce computing time.

ARTICLE INFO

Article history:
Received 8 August 2013
Accepted 10 October 2013
Available online 22 October 2013

Keywords:
Underground air tunnel
Transportation tunnel
Geothermal energy
Numerical
Heat transfer

ABSTRACT

Underground tunnels used in underground constructions serve as huge ventilation pipes that conduct outside fresh air into a cavern. Predicting the heat and mass transfer is critically important in order to exploit the relatively constant underground soil temperature for heat transfer, and to ensure sufficient ventilation for occupational safety. This paper presents a numerical model developed to describe the simultaneous heat transfer between air and the tunnel surface, taking into account the condensation phenomena inside the tunnel. The soil surrounding the tunnel is treated as an equivalent long annulus and divided into several cross-section slices. With appropriate assumptions, a set of discrete numerical equations and its solution is proposed. The developed model is validated against field measurements which showed good agreement between the simulated results and measurement data. The model is then applied to an underground tunnel operating for a ten-year-period.

1. Introduction

In many underground constructions, tunnels are needed for transportation and access to and from the outer ground surface, while at the same time serves as a huge ventilation pipe to conduct outside fresh air into the underground cavern. This kind of tunnels are often found in underground hydropower stations (Fig. 1) and extend for long distances up to 1000 m and buried deep underground. At a sufficient depth, (typically 4 m or greater [1]) the tunnel takes advantage of relatively constant soil temperature despite the outside seasonal weather changes. This allows both cooling for the underground ground constructions during hot weather, and heating in winter [2]. Its high cooling and heating potential result in a major reduction in energy consumption and initial investment making the transportation tunnel highly beneficial and cost-effective in underground constructions [3–7]. Furthermore it provides the required fresh air to all underground work areas in sufficient amounts to prevent dangerous or harmful accumulation of dusts, fumes, or gases.

This paper focuses on the heat and mass transfer within an underground transportation tunnel. Physically, the energy performance of an underground tunnel is a transient heat conduction–convection problem, influenced by multi-factors. Besides heat transfer to and from the air, condensation of air should also be considered. This developed model can also provide accurate predictions of air parameters at the outlet, including air temperature and relative humidity, which are critical parameters in determining the energy conservation potential of a tunnel.

The energy performance of underground tunnel systems has been investigated through analytical and numerical models. Ben and Kanoun [8] studied the cooling and heating effect of underground heat pipes using a thermal resistance method to evaluate the thermal capacities. Krarti and Kreider [9] used a simplified analytical model which assumed that all variations are periodic

* Corresponding author. Tel.: +86 23 6512 0756; fax: +86 23 6512 7539.
E-mail addresses: xiaoyimin@cqu.edu.cn, xiaoyimin1974@126.com (Y. Xiao).

1359-4311/$ – see front matter © 2013 Elsevier Ltd. All rights reserved.
http://dx.doi.org/10.1016/j.applthermaleng.2013.10.017

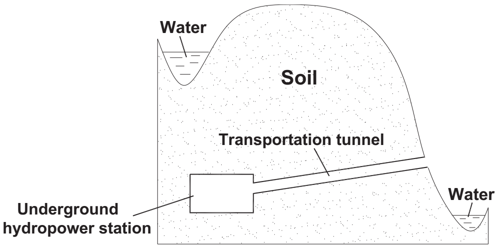

Fig. 1. Schematic of a deeply buried underground tunnel used at underground Hydropower Stations, China.

functions of time. However, a limitation of this study is that it does not consider condensation and therefore cannot predict the moisture content of the circulating air. Recently Cucumo et al. [10] proposed an analytical model which considers condensation, but this is realized by using a pre-assumed quadratic profile.

An alternate approach is the discrete numerical model. Based on this, Mihalakakou et al. [11] proposed a model validated with long-term measurements to describe the thermal influence of key variables such as length, diameter and air velocity. Wu and Wang [12] also proposed a numerical model to predict the thermal performance and cooling capacity of underground soil to air systems. Hokoi et al. [13] developed an approximate two dimensional model of an underground rectangular tube to produce a solution nearly equal to that of a three dimensional model. However these models do not consider moisture condensation and latent heat transfer. Su et al. [14] proposed a numerical model which calculated both air temperature and relative humidity, but the mass transfer coefficient is assumed as this is difficult to determine.

In this paper, a simplified and efficient numerical model is proposed, which calculates the air flow temperature, and accounts for condensation. With appropriate simplifications, the discrete numerical equations and computing procedure, is proposed for calculation efficiency and computation time. The results obtained by the model are validated against field measurement data. Finally, the developed model is applied to an underground tunnel system and modeled for a ten-year-period.

2. Mathematical model formulation

2.1. Heat conduction through underground soil

The conduction heat transfer from the tunnel walls through the underground soil is treated as an equivalent long cylinder where its spatial dimensions are defined in cylindrical coordinates (Fig. 2). Taking thin circular cross-section slices of the tunnel and surrounding soil, the general 3D heat conduction equation acting radially through each slice is simplified as a 1D problem in cylindrical coordinates when the following conditions are met:

i) The heat transfer across the thickness, Δz is small in comparison to radial direction, r, therefore the temperature variation in the Δz can also be assumed constant in comparison to the radial temperature variation [3,14]. The variation across r is very large since r reaches a maximum of 10 m.
ii) The temperature distribution along its azimuth or angular coordinate φ, is treated as constant, if its variation is very small in comparison to the variation in the radial direction, r of the surrounding soil [15].
iii) Field measurements were obtained at underground tunnels service the Hydropower Stations in China. These tunnels are at an average underground depth of 50 m and 70 m respectively. Therefore the influence of the surface temperature is neglected and the initial soil temperature is considered uniform and without any gradients [9].

The heat conduction occurring radially through each thin soil section is given by

$$\frac{\partial T}{\partial t} = \frac{k}{\rho C_p}\left(\frac{\partial^2 T}{\partial r^2} + \frac{1}{r}\frac{\partial T}{\partial r}\right) \tag{1}$$

where, T is the temperature variation within the soil, [°C]; t is time, [s]; k is soil thermal conductivity, [W/m °C]; ρ is soil density, [kg/m^3]; C_p is the soil specific heat, [kJ/kg °C] and r is the radius. The air tunnel geometry specifications are 1000-m-long, and $r_{max} = 10$ m, and an optimum value of $\Delta z = 10$ m, which produces 100 thin soil sections. During the numerical solution, the influence of Δz thickness was evaluated, with thickness of 1 m to 10 m and this is discussed in the results. The air tunnel surface has thickness between 0 and 200 mm, which is much smaller when compared with soil radius (10 m). The material is primarily concrete density of 2344 kg/m^3, specific heat of 750 J/kg °C and thermal conductivity of 1.84 W/m °C which is similar to underground soil. Therefore, the surface produces a low thermal resistance and is neglected in this work. This means that there is a direct interface between air tunnel and the underground soil using a common temperature $T_{surface}$.

2.2. Energy conservation equation of air stream in the air-tunnel

The air stream moving through the tunnel from the inlet to the outlet experiences a variation in temperature and relative humidity as it is heated or cooled within the length of the tunnel. Similarly, the moisture content of air will also change. When warmer air comes into contact with a cooler tunnel surface temperature, sufficiently enough to drop its temperature to dew point, condensation occurs and consequently its moisture content decreases. Another factor to consider is any significant water seepage on the tunnel surface which results in water evaporating from the tunnel surface into air, causing an increase in the air moisture content. However, field measurements and observations showed that the tunnel surface had been treated with anti-seepage technology reducing the moisture evaporation from the tunnel surface into the air. Therefore, evaporation is neglected and only condensation is considered in this paper. This assumption allows further simplifications of the model to obtain a feasible calculation of the underground tunnel system.

Under the assumption of constant air properties on the cross section, the variation in the air properties is considered as a 1D problem along the cross-section thickness, (Δz). The energy conservation equation is written as:

$$\dot{m}\left(C_{p,air}\frac{\partial T_{air}}{\partial z} + L\frac{\partial u_w}{\partial z}\right) = \dot{Q} \tag{2}$$

where $\dot{m}$ is air flow rate, kg/s; $C_{p,air}$ is specific heat of air, [J/kg °C]; T_{air} is air temperature, [°C]; z is the axial coordinate, [m]; L is the latent heat of moisture, [J/kg]; u_w is the air moisture content; $\dot{Q}$ is the convection heat transfer rate between air and tunnel surface, [J/s], which is simply defined without condensation as

$$\dot{Q} = hA\left(T_{air} - T_{surf}\right) \tag{3}$$

T_{surf} is the surface temperature of the tunnel, [°C]; A is the heat transfer area, [m^2]; h is the convective heat transfer coefficient, [W/m^2 K] which is determined from Ref. [16] as

$$h = 0.023\frac{k_{air}}{D_h}\mathrm{Re}^{0.8}\mathrm{Pr}^n \tag{4}$$

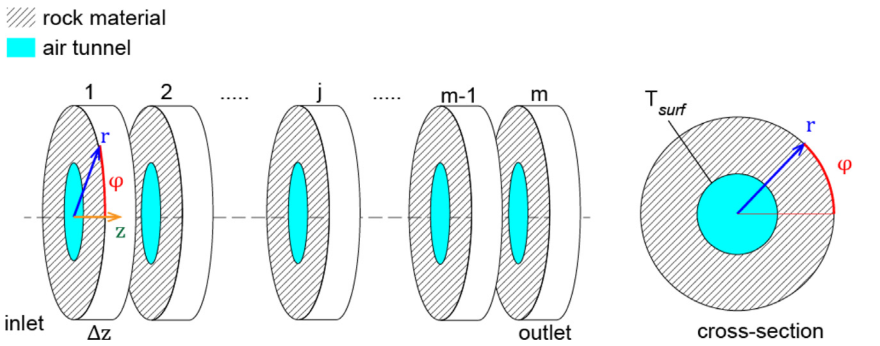

Fig. 2. Radial cross-sections of the earth soil surrounding the air-tunnel using cylindrical coordinates. Each cross-section is labeled from 1 to m, and has thickness Δz, where $\Delta z << r$. T_{surf} is the temperature at the surface of the tunnel.

k_{air} is air thermal conductivity, [W/(m °C]; D_{h} is the hydraulic diameter, [m]; n is an index which is 0.4 when air is heated and 0.3 for cooling.

In the case of condensation, $\dot{Q}$ is determined by the Lewis [3] approach and given by:

$$\dot{Q} = \frac{hA}{C_{\text{p,air}}}\left(h_{\text{air}} - h_{\text{surf}}\right) \tag{5}$$

where h_{air} is the specific enthalpy of air, [J/kg]; h_{surf} is the specific enthalpy of the air layer on the tunnel surface at the surface temperature and saturated humidity.

2.3. Air equations of state

Other thermodynamic properties of the air, including relative humidity and moisture content will be affected by the variation in air temperature. Therefore, the air equations of state are included to define the relationship between temperature, relative humidity and moisture content. When condensation occurs, air will reach a saturated state and its relative humidity will remain constant whereas neglecting condensation the relative humidity will vary with temperature. Therefore, the air equations of state are defined by Eq. (6) based on Su et al. [14].

$$\begin{cases} \frac{\partial \varphi_{\text{RH}}}{\partial z} = 0 \ \ (\text{with condensation}) \\ \frac{\partial u_{\text{w}}}{\partial z} = 0 \ \ (\text{without condensation}) \\ \varphi_{\text{RH}} = \frac{u_{\text{w}}P}{f(T')(0.622+u_{\text{w}})} \end{cases} \tag{6}$$

where, φ_{RH} is relative humidity; T' is the thermodynamic temperature of air, K; P is local atmospheric pressure, Pa. The function $f(T')$ defines the thermodynamic temperature, which is given as

$$f(T') = \exp\left[C_1(T')^{-1} + C_2 + C_3T' + C_4(T')^{-1} + C_5(T')^{-1} + C_6\ln(T')\right] \tag{7}$$

where, $C_1 = -5800.2206$, $C_2 = 1.3914993$, $C_3 = -0.04860239$, $C_4 = 0.41764768 \times 10^{-4}$, $C_5 = -0.14452093 \times 10^{-7}$, $C_6 = 6.5459673$.

2.4. Boundary conditions

The heat transfer between the air and tunnel surface is described by the convection heat transfer equation. The corresponding boundary condition is given by Eq. (8)

$$\dot{Q} = -k\left(\frac{\partial T}{\partial r}\right)\Big|_{\text{surface}} \tag{8}$$

where the subscript surface represents the air tunnel surface and soil interface; $(\partial T/\partial r)|_{\text{surface}}$ is the temperature gradient at rock-tunnel surface interface, 1/°C.

Under real applications, periodic variation of the air temperature arises from seasonal change in the environment (Fig. 3). This results in variations in the heat transfer between the circulating air and underground soil but this effect is limited to a certain distance found to be ≈10 m from the tunnel surface [9]. Radial distances greater than 10 m away from the tunnel surface remain constant. Therefore, this distance is considered as an external boundary and treated as constant temperature condition as

$$T(r) = C \quad \text{for} \ \ r = 10 \text{ m}$$

For air properties at the tunnel inlet, values are obtained from field measurement and local weather database. Field tests were carried out to provide both boundary condition values and validation data for the results of the proposed numerical model. Two field measurements were undertaken at different locations and labeled as Tunnel A and Tunnel B, both of which are transportation tunnels in an underground hydropower station (details are given in Table 1). Tunnel A is located at 2100 m above sea level, which causes the local average atmospheric pressure to be 83.76 kPa. While tunnel B is located at 43.9 m above sea level giving a local

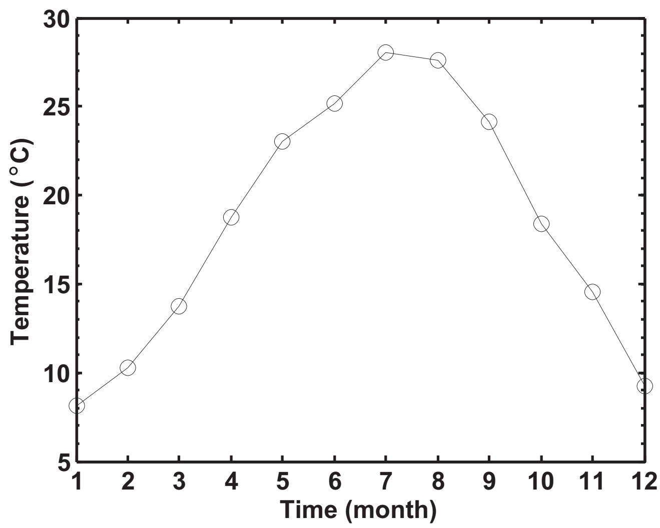

Fig. 3. Seasonal temperature change in Chongqing, China.

average atmospheric pressure of 101.86 kPa. Tunnel A is shorter at 310 m in length while Tunnel B is a longer at 1104 m, and both have a sufficient average depth to ensure the soil around the tunnel will not be affected by any ground surface temperature fluctuation. The internal surface of the two tunnels was found to be dry with negligible water seepage, which satisfies Eq. (6).

For Tunnel A, air temperature and relative humidity were measured while for Tunnel B, inlet air temperature and relative humidity were measured, and only air temperature was measured for the inside cross sections. The specific position (z) of each measured cross section for Tunnel A are: 30, 60, 90, 120, 150, 180, 210, 230, 260 and 310 m and; for Tunnel B: 30, 60, 90, 170, 340, 510, 680, 850, 990 and 1000 m. The air temperature and relative humidity were recorded by automatic data loggers while air velocity was measured by a thermal anemometer manually.

3. Discretized equations

The underground air tunnel geometry is discretized into a computational domain through uniformly distributed nodes in both the radial and axial coordinate (Fig. 4). Nodes in the radial coordinate have an interval of Δr and are limited to the soil domain. The nodes are labeled from $i = 1$ to n where $i = 1$ is the external soil boundary, and $i = n$ is the air tunnel surface. Nodes in the axial coordinate have an interval of Δz and are limited to the air tunnel domain. The nodes represent cross-section slices depicted in Fig. 2 and are labeled from $j = 1$ to m where $j = 1$ is the inlet cross-section and $j = m$ is the outlet cross-section.

3.1. Nodes in underground soil

The differential equations (Eqs. (1)–(8)) are discretized using the finite difference method. Using a time step of Δt, and applying the central difference scheme Eq. (1) becomes

$$T_i^{t+1} = (M+N)T_{i-1}^t + (1-2M)T_i^t + (M-N)T_{i+1}^t \quad (\text{for } i = 2 \text{ to } i = n-1) \tag{9}$$

where $M = \frac{k\Delta t}{\rho C_p (\Delta r)^2}$, $N = \frac{k\Delta t}{2\rho C_p \Delta r[(n-i)\Delta r + R]}$.

3.2. Nodes in air-tunnel

In the air tunnel it is assumed that the variation of the air properties is caused by the heat transfer from the preceding cross-section slice ($j - 1$) and therefore, the heat transfer occurs sequentially through each cross-section slice.

If there is condensation in the previous slice the relative humidity remains constant in the subsequent slice while the moisture content decreases. For the no-condensation case the relative humidity changes with temperature and the moisture content is constant. According to Eqs. (2) and (6), the air parameters in the subsequent cell is obtained by

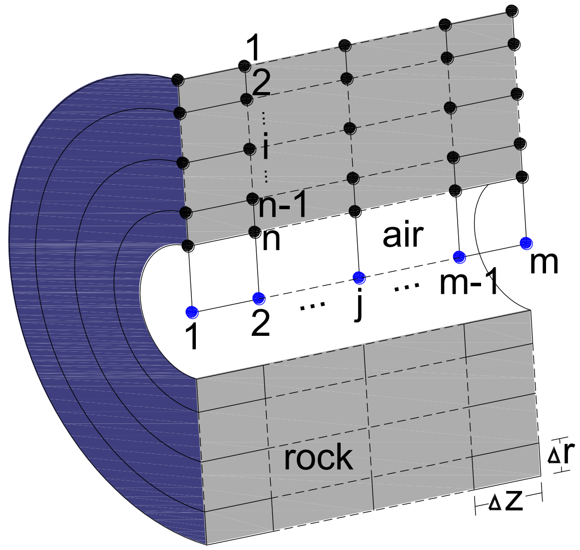

Fig. 4. Discretization of the physical tunnel domain into a numerical mesh.

$$\begin{cases} T^t_{\mathrm{air},j+1} + \frac{L}{C_{\mathrm{p,air}}}\left(u^t_{\mathrm{w},j+1} - u^t_{\mathrm{w},j}\right) = -\frac{\Delta z}{\dot m C_{\mathrm{p,air}}}\dot Q + T^t_{\mathrm{air},j} \\ \varphi^t_{\mathrm{RH},j+1} = \varphi^t_j = 1 \quad (\text{with condensation}) \\ u^t_{\mathrm{w},j+1} = u^t_{\mathrm{w},j} \quad (\text{without condensation}) \\ \varphi^t_{\mathrm{RH},j+1} = \frac{u^t_{\mathrm{w},j+1} P}{f\left(T^{t,k}_{j+1}\right)\left(0.622 + u^t_{\mathrm{w},j+1}\right)} \end{cases} \tag{10}$$

where $\dot Q$ is:

$$\begin{cases} \dot Q = hA\left(T^t_{\mathrm{air},j} - t^t_n\right) \quad (\text{without condensation}) \\ \dot Q = \frac{hA}{C_{\mathrm{p,air}}}\left(h^t_{\mathrm{air},j} - h^t_{\mathrm{surf},j}\right) \quad (\text{with condensation}) \end{cases} \tag{11}$$

3.3. Boundary nodes

The boundary condition for $i = n$ is obtained from Eq. (8), which gives:

$$T_n^{t+1} = E\dot Q + (1-E-F)T_n^t + EFT_{n-1}^t \tag{12}$$

where, $E = \frac{4\Delta t}{\Delta r(4R+\Delta r)\pi\rho C_p}$, $F = 2\pi k\left(\frac{R}{\Delta r} + \frac{1}{2}\right)$, $\dot Q$ is obtained from Eq. (11).

The far external soil boundary at $i = 1$ is treated as a constant temperature defined as

$$T_1^{t+1} = T_0 \tag{13}$$

where T_0 is the initial deep underground temperature, °C.

The inlet boundary conditions for the air tunnel section is defined according to measured or the local weather data. This means that the air properties in the first cross-section $j = 1$ cell are considered as known values, defined as

Table 1
Details of measured tunnel.

Parameter	Values	
	Tunnel A	Tunnel B
Length (m)	310	1104
Average depth (m)	50	70
Local atmospheric pressure (kPa)	83.76	101.86
Diameter (m)	6.8	8.18
Soil thermal conductivity (W/(m K))	2.8	2.92
Soil specific heat (J/(kg/K))	900	660
Soil density (kg/m^3)	3080	2820
Air flow rate (m^3/s)	72	58.8
Internal surface situation	Dry	Dry
Annual average air temperature (°C)	16.9	11.6
Testing time	July 16–July 21	Aug 30–Sep 2

$$\begin{cases} T^t_{\mathrm{air},1} = T_{\mathrm{air}}(t) \\ \phi^t_{\mathrm{RH},1} = \phi_{\mathrm{RH}}(t) \end{cases} \tag{14}$$

$T_{\mathrm{air}}(t)$ and $\phi_{\mathrm{RH}}(t)$ are the hourly temperature and relative humidity values based on the measured and local weather data.

3.4. Numerical solution

Fig. 5 shows the computational procedure which solves the discretized equations sequentially. The solution is initialized with the known values at the first cross-section cell, $j = 1$. The computation starts at $t = t_0$ from the first cross-section slice. Air parameters in the first cross-section slice are defined with known values and the initial soil temperature distribution is set to the annual air temperature from the local weather data. After computation in the first cross-section slice (j), the air parameters are transferred to the next slice ($j + 1$). The soil temperature distribution in the first slice is calculated through the discretized conduction equation based on the tunnel surface temperature, T_{surface} at time t_0. This temperature distribution is then used as the initial profile for the next time step, $t + 1$. When all cross-section slices are finished sequentially (looping through j number of cells), the computations move to the next time step and the calculations restarts at the inlet cross-section cell $j = 1$ again. The air parameters in the tunnel section slices are updated every time step based on the inlet air parameters. Other parameters, such as velocity and convection coefficient, are also updated at every time step correspondingly.

3.5. Underground soil temperature initialization

The initial soil temperature distribution has a great influence on the calculated results due to the climatic temperature variation of the outer air impacting entering the tunnel inlet, and also the convection heat transfer through the air tunnel and conduction through the soil. Therefore, it is not possible to accurately determine the initial rock temperature distribution. In order to setup the initial temperature distribution to replicate the field measurements, the follow method is used. For long term calculations, the influence of the initial conditions are negligible if the start-up effect of unsteady modeling is allowed to dissipate over the long period of time. Therefore the soil temperature is initially set to a uniform value, based on the local annual average air temperature and allowed to reach equilibrium over time. The inlet air properties obtained from local weather database are used to run the calculations for a period of six-months to allow the non-uniform soil temperature distribution to be obtained. After this period, the measurement data is used to validate the numerical model.

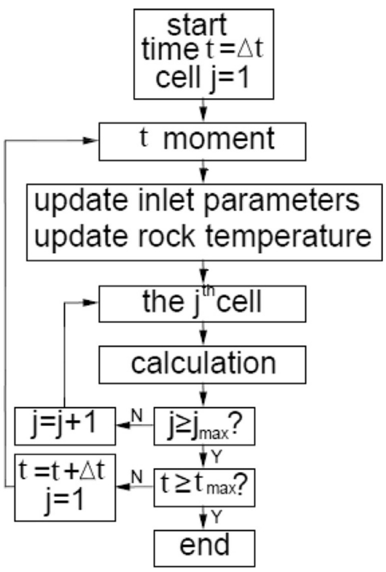

Fig. 5. Computation procedure. The spatial discretization are $\Delta r = 0.05$ m, $\Delta z = 10$ m with time steps of $\Delta t = 300$ s.

4. Validation of numerical models

First the grid independence validation was carried out, two models with different mesh density were tested. The mesh setting for model 1 is: $\Delta r = 0.05$ m; $\Delta z = 10$ m; $\Delta t = 300$ s. For model 2, the setting is: $\Delta r = 0.01$ m; $\Delta z = 1$ m; $\Delta t = 50$ s. The hourly outlet temperature and humidity values between the two simulations were different by1.6×10^{-4} °C and 0.008%, respectively. Model 1 was found to be sufficient, to reduce computation size and calculation time. Therefore, all mesh settings in this paper are that of model 1.

4.1. Tunnel A

In Tunnel A, the air temperature and relative humidity at a cross-section near the tunnel outlet $z = 260$ m ($z/L = 0.84$) are

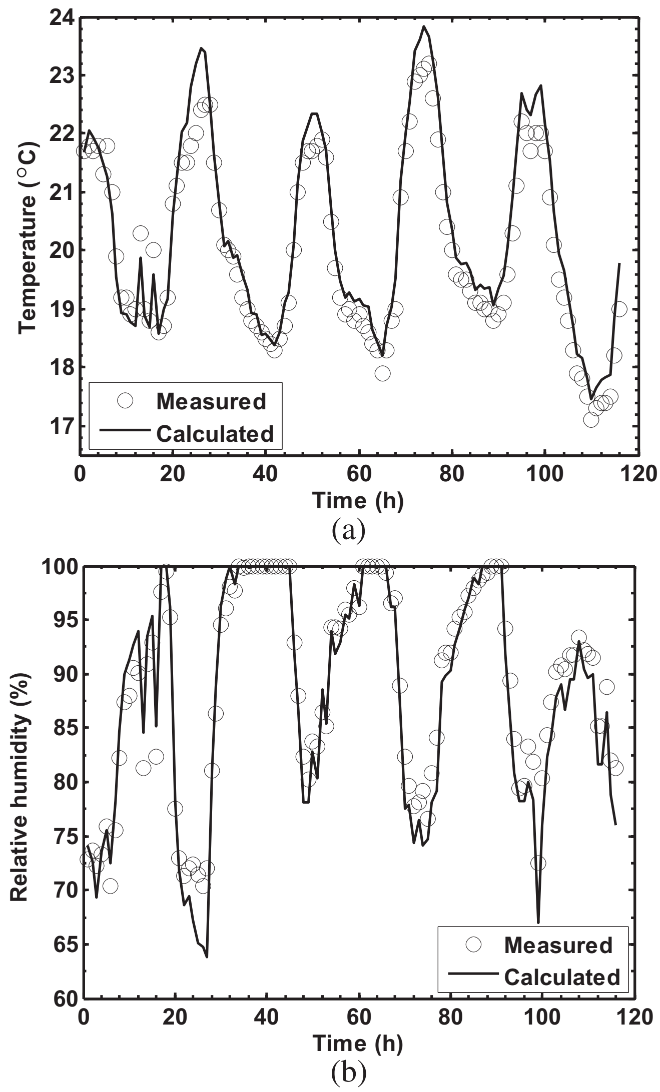

Fig. 6. Comparison of air properties at $z = 260$ m ($z/L = 0.84$) cross section (a) average cross-section temperature (b) average cross-section relative humidity.

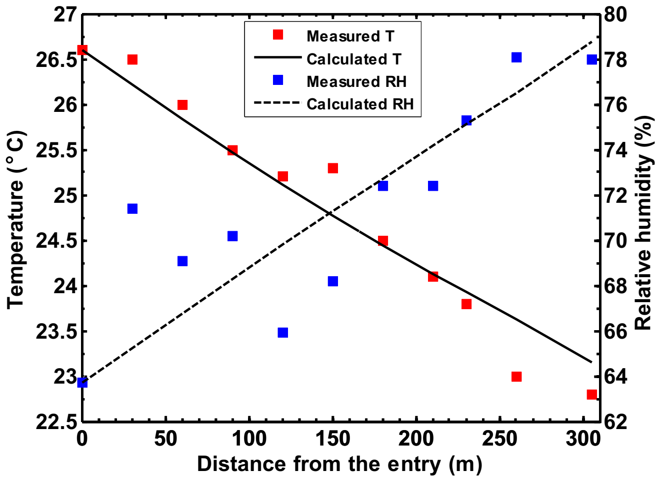

Fig. 7. Comparison of air temperature and relative humidity along the tunnel.

compared in Fig. 6a and b. The comparison shows reasonable agreement between the numerical and field measurement data. Fig. 6a shows the maximum discrepancy between the prediction and measured data is 1.19 °C. The maximum discrepancy in relative humidity calculation is 8.22%. The measured data shows that the air stream in Fig. 6b reaches a saturated state and condensation occurs. Meanwhile, the same phenomenon is captured by the numerical model, which suggests that the assumptions of the model are valid for considering the condensation process.

Fig. 7 is the temperature and relative humidity comparison along the axial direction, Δz at 15:00 in July the 6th. It shows that the air is cooled as it flows through the tunnel. The maximum discrepancy in the predicted temperature and relative humidity is 0.62 °C and 6.19%, respectively.

In this paper, it is assumed that the heat transfer inside the soil along Z direction is small, and is ignored. After calculation, the average soil temperature change along Z direction (from 0 m to 310 m) is only 0.1 °C, which supports the previous assumption.

4.2. Tunnel B

In Tunnel B, the air temperature at $z = 30$ m ($z/L = 0.027$), 510 m ($z/L = 0.46$) and 1000 m ($z/L = 0.91$) are compared in Fig. 8. The

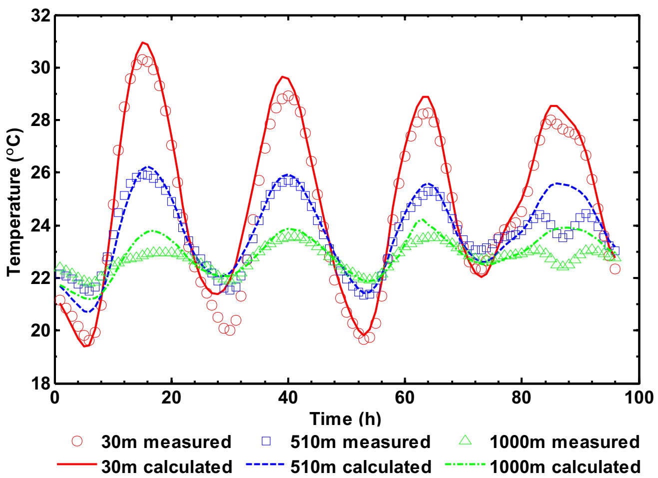

Fig. 8. Comparison of air temperature at different cross sections at $z = 30$ ($z/L = 0.027$), $z = 510$ m ($z/L = 0.46$) and $z = 1000$ m ($z/L = 0.91$).

results indicate that the air fluctuation reduces with tunnel distance from the inlet and that both heating and cooling occur. The field measurements were undertaken during the summer season, and during day time, the inlet air temperature is higher than that of the tunnel surface. Heat is transferred from the air to soil and stored in the soil causing an increase in the underground soil temperature. During night time, the air stream is heated because of the low inlet temperature at night. The heat in the soil is released back into the air. Therefore, the heat transfer between air and soil is a dynamic cyclic process.

During measurements, ventilation at the experimental site ceased during the period $t = 81$–91 h in field measurement shown in Fig. 8, which influences the comparisons between the numerical result and the field measurement. Besides this, the simulated values fit the measured values well. The maximum calculation error is 2.18 °C, and average calculation error is 0.34 °C.

Fig. 9a and b are the temperature comparison along the axial direction, Δz, at 14:00 in Aug 30th and 4:00 in Sep 1st. Fig. 9a shows that the air is being cooled and the measured temperature drop from inlet to outlet is 8.5 °C, while the numerical model predicted a value of 7.7 °C. During night time shown in Fig. 9b, the air is heated with measured and simulated temperature increase of 2.28 °C and

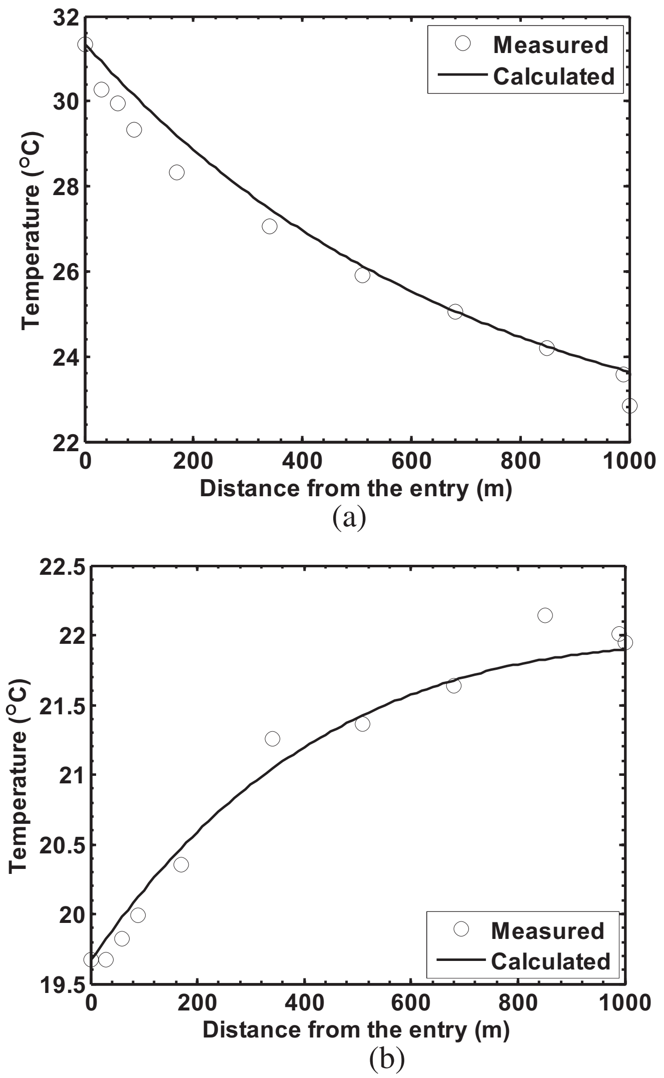

Fig. 9. Comparison of air temperature along the tunnel (a) comparison at 14:00 in Aug the 30th (b) comparison at 4:00 in Sep the 1st.

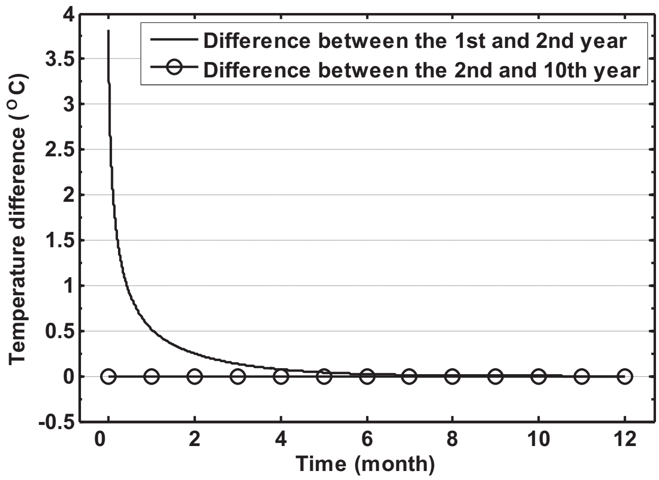

Fig. 10. Outlet temperature difference between two selected years.

2.23 °C respectively. The calculated values are in good agreement with the measured values, which indicate that the numerical model can accurately calculate the dynamic heat transfer process.

5. Case study

A case study is presented to highlight the applicability of the proposed numerical model. A deeply buried underground tunnel with a length of 1000 m having soil properties of thermal conductivity $k = 2$ W/(m K); specific heat $C_p = 950$ J/(kg/K) and density $\rho = 2500$ kg/m^3 is used. The radius of the equivalent cylinder tunnel is 4 m and the air stream velocity is 1 m/s. The hourly inlet air properties are based on local weather database gathered in the city of Chongqing, China and the initial calculation date is started at Jan 1st. The initial temperature of the rock is assumed to be uniformly distributed with an averaged local underground soil temperature. The influence of the initial boundary conditions is shown in Fig. 10, where the outlet temperature value taken for the first year of simulated results is compared with the second year of results. The results show that a temperature variation occurs in the first six months of the first simulation year which is caused by the initial uniform soil temperature distribution causing the associated start-up effect that occurs for of any time-dependent simulation. After the six months, the soil temperature distribution is established and the outlet temperature between any two consecutive years shows a negligible value.

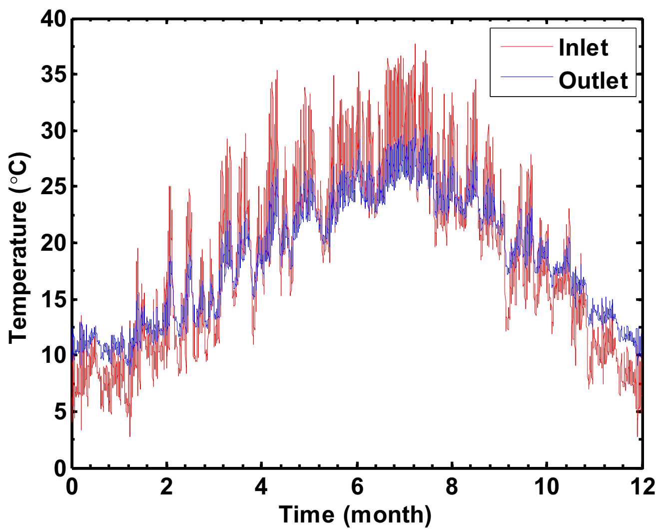

Fig. 11. Inlet and outlet hourly air temperature at the 10th year.

Fig. 11 is the inlet and outlet air temperature value in the 10th year, which shows that the air stream is cooled in summer, but there is a small amount of time in the night that the air stream is heated. The opposite phenomenon occurs in winter. During a whole year of simulation time, the average and maximum temperature drop of air stream in summer is 2.35 °C and 8.93 °C, respectively, while the average and maximum temperature increase in the air stream is 2.13 °C and 6.27 °C respectively in winter for heating condition.

6. Conclusion

(1) A simplified numerical model is developed for ventilation of transportation tunnels in underground hydropower stations, which takes into account both temperature and condensation. This model, avoids the introduction of a mass transfer coefficient which greatly simplifies the computational difficulty and reduces computational time.
(2) Besides an underground hydropower station, this model can also be used in deeply buried tunnels of any underground constructions, particularly those serving heat exchange piping networks. This model is also suitable for any deeply buried earth–air–pipe systems, where axial distance between pipes is large enough to avoid thermal interference.
(3) The discrete numerical equations and computing procedure are given in detail, can quickly solve the heat and mass transfer problem and greatly improve the computational efficiency. For instance, the computational time of a tunnel with 1000 m long for one-year-period simulation is only 6 min based on today's personal computer. Therefore this model is highly suited for industry use.
(4) Field measurements were carried out to validate the simulation result of a simplified model. For Tunnel A, the maximum deviation of air temperature and relative humidity is 1.19 °C and 8.22%, respectively. Meanwhile, the model can accurately calculate the condensation phenomenon. For Tunnel B, the maximum deviation of the calculation result at different cross-section is 2.18 °C, and average deviation is 0.34 °C.
(5) The simplified model is also used to carry out a ten-year simulation period. The result shows that the impact of initial rock temperature will disappear after a half year of simulation. The air stream is mainly cooled in summer and heated in winter, and the average temperature drop in summer and temperature rise in winter is 2.35 °C and 2.13 °C, respectively.

Acknowledgements

The work presented in this paper is financially supported by National Nature Science Foundation of China (Project No. 51178482), Fundamental Research Funds for the Central Universities (Project No. CDJZR11 21 00 04) and China Scholarship Council (CSC: 201206050088).

References

[1] S.S. Bharadwaj, N.K. Bansal, Temperature distribution inside ground for various surface conditions, Building Environ. 16 (1981) 183–192.
[2] R. Kumar, S. Ramesh, S.C. Kaushik, Performance evaluation and energy conservation potential of earth–air–tunnel system coupled with non-air-conditioned building, Building Environ. 38 (2003) 807–813.

[3] P. Hollmuller, B. Lachal, Cooling and preheating with buried pipe systems: monitoring, simulation and economic aspects, Energy Buildings 33 (2001) 509–518.
[4] M. Maerefat, A.P. Haghighi, Passive cooling of buildings by using integrated earth to air heat exchanger and solar chimney, Renewable Energy 35 (2010) 2316–2324.
[5] M. Santamouris, G. Mihalakakou, D.N. Asimakopoulos, On the coupling of thermostatically controlled buildings with ground and night ventilation passive dissipation techniques, Solar Energy 60 (1997) 191–197.
[6] J.W. Stevens, Optimal placement depth for air–ground heat transfer systems, Appl. Therm. Eng. 24 (2004) 149–157.
[7] B. Stojanović, J. Akander, Build-up and long-term performance test of a full-scale solar-assisted heat pump system for residential heating in Nordic climatic conditions, Appl. Therm. Eng. 30 (2010) 188–195.
[8] H. Ben Jmaa Derbel, O. Kanoun, Investigation of the ground thermal potential in tunisia focused towards heating and cooling applications, Appl. Therm. Eng. 30 (2010) 1091–1100.
[9] M. Krarti, J.F. Kreider, Analytical model for heat transfer in an underground air tunnel, Energy Convers. Manage. 37 (1996) 1561–1574.
[10] M. Cucumo, S. Cucumo, L. Montoro, A. Vulcano, A one-dimensional transient analytical model for earth-to-air heat exchangers, taking into account condensation phenomena and thermal perturbation from the upper free surface as well as around the buried pipes, Int. J. Heat Mass Transfer 51 (2008) 506–516.
[11] G. Mihalakakou, M. Santamouris, D. Asimakopoulos, I. Tselepidaki, Parametric prediction of the buried pipes cooling potential for passive cooling applications, Solar Energy 55 (1995) 163–173.
[12] H. Wu, S. Wang, D. Zhu, Modelling and evaluation of cooling capacity of earth–air–pipe systems, Energy Convers. Manage. 48 (2007) 1462–1471.
[13] S. Hokoi, S. Ueda, T. Yoshida, Cooling effect of cool tube-part 1: evaluation of cooling effect without moisture transfer, ASHRAE Trans. 104 (1998).
[14] H. Su, X.-B. Liu, L. Ji, J.-Y. Mu, A numerical model of a deeply buried air–earth–tunnel heat exchanger, Energy Buildings 48 (2012) 233–239.
[15] A. Tzaferis, D. Liparakis, M. Santamouris, A. Argiriou, Analysis of the accuracy and sensitivity of eight models to predict the performance of earth-to-air heat exchangers, Energy Buildings 18 (1992) 35–43.
[16] A. de Jesus Freire, J.L. Coelho Alexandre, V. Bruno Silva, N. Dinis Couto, A. Rouboa, Compact buried pipes system analysis for indoor air conditioning, Appl. Therm. Eng. 51 (2013) 1124–1134.